RESEARCH ARTICLE

The *Cryptococcus neoformans* Transcriptome at the Site of Human Meningitis

Yuan Chen,[a] Dena L. Toffaletti,[a] Jennifer L. Tenor,[a] Anastasia P. Litvintseva,[b]* Charles Fang,[a] Thomas G. Mitchell,[b] Tami R. McDonald,[c] Kirsten Nielsen,[c] David R. Boulware,[c] Tihana Bicanic,[d] John R. Perfect[a,b]

Division of Infectious Diseases, Department of Medicine[a] and Department of Molecular Genetics and Microbiology,[b] Duke University Medical Center, Durham, North Carolina, USA; Department of Microbiology and Medicine, University of Minnesota, Minneapolis, Minnesota, USA[c]; St. George Hospital, London, England[d]

* Present address: Anastasia P. Litvintseva, Mycotic Diseases Branch, Centers for Disease Control and Prevention, Atlanta, Georgia, USA.

ABSTRACT ***Cryptococcus neoformans*** **is the leading cause of fungal meningitis worldwide. Previous studies have characterized the cryptococcal transcriptome under various stress conditions, but a comprehensive profile of the *C. neoformans* transcriptome in the human host has not been attempted. Here, we extracted RNA from yeast cells taken directly from the cerebrospinal fluid (CSF) of two AIDS patients with cryptococcal meningitis prior to antifungal therapy. The patients were infected with strains of *C. neoformans* var. *grubii* of molecular type VNI and VNII. Using RNA-seq, we compared the transcriptional profiles of these strains under three environmental conditions (*in vivo* CSF, *ex vivo* CSF, and yeast extract-peptone-dextrose [YPD]). Although we identified a number of differentially expressed genes, single nucleotide variants, and novel genes that were unique to each strain, the overall expression patterns of the two strains were similar under the same environmental conditions. Specifically, yeast cells obtained directly from each patient's CSF were more metabolically active than cells that were incubated *ex vivo* in CSF. Compared with growth in YPD, some genes were identified as significantly upregulated in both *in vivo* and *ex vivo* CSF, and they were associated with genes previously recognized for contributing to pathogenicity. For example, genes with known stress response functions, such as *RIM101*, *ENA1*, and *CFO1*, were regulated similarly in the two clinical strains. Conversely, many genes that were differentially regulated between the two strains appeared to be transporters. These findings establish a platform for further studies of how this yeast survives and produces disease.**

IMPORTANCE ***Cryptococcus neoformans*****, an environmental, opportunistic yeast, is annually responsible for an estimated million cases of meningitis and over 600,000 deaths, mostly among HIV-infected patients in sub-Saharan Africa and Asia. Using RNA-seq, we analyzed the gene expression of two strains of *C. neoformans* obtained from the cerebrospinal fluid (CSF) of infected patients, thus creating a comprehensive snapshot of the yeasts' genetic responses within the human body. By comparing the gene expression of each clinical strain under three conditions (*in vivo* CSF, *ex vivo* CSF, and laboratory culture), we identified genes and pathways that were uniquely regulated by exposure to CSF and likely crucial for the survival of *C. neoformans* in the central nervous system. Further analyses revealed genetic diversity between the strains, providing evidence for cryptococcal evolution and strain specificity. This ability to characterize transcription *in vivo* enables the elucidation of specific genetic responses that promote disease production and progression.**

Received 17 December 2013 **Accepted** 23 December 2013 **Published** 4 February 2014

Citation Chen Y, Toffaletti DL, Tenor JL, Litvintseva AP, Fang C, Mitchell TG, McDonald TR, Nielsen K, Boulware DR, Bicanic T, Perfect JR. 2014. The *Cryptococcus neoformans* transcriptome at the site of human meningitis. mBio 5(1):e01087-13. doi:10.1128/mBio.01087-13.

Editor Françoise Dromer, Institut Pasteur

Address correspondence to John R. Perfect, perfe001@mc.duke.edu.

Cryptococcus neoformans is an environmental, encapsulated yeast and major opportunistic, neurotropic pathogen. Patients with low levels of $CD4^+$ lymphocytes are particularly susceptible. In sub-Saharan Africa, the epicenter of the AIDS pandemic, *C. neoformans* is annually responsible for an estimated million cases of meningoencephalitis and approximately 600,000 deaths (1). Over the past 30 years, many molecular and phenotypic studies have identified a cohort of *C. neoformans* genes that clearly enhance but are not necessarily sufficient for virulence, such as the capsular polysaccharide, the ability to grow at 37°C, and the production of melanin, urease, phospholipase, and other factors (2). With the availability of genomic sequences, more recent studies have begun to analyze the transcriptome of *C. neoformans* under conditions that pertain to its pathogenicity (3–7). Using well-characterized laboratory strains of *C. neoformans*, reports have documented the transcriptional responses to high-temperature (8, 9), nitric oxide (9), iron (10), capsule-inducing conditions (11, 12), antifungal drugs (13), and survival within macrophages (14) and murine lungs (15). However, the transcriptional responses to stresses are dynamic and react to a variety of signals. To investigate the signals, transcription factors, and genes that enable *C. neoformans* to cause disease, it is critical to identify the genes that are transcribed by *C. neoformans* in the central nervous system (CNS). In addition, since most molecular transcrip-

TABLE 1 Number of RNA-seq reads obtained for each sample and mapping results

Characteristic	G0			HC1		
	YPD	*Ex vivo* CSF	*In vivo* CSF	YPD	*Ex vivo* CSF	*In vivo* CSF
Sequencing type	Single end	Paired end	Single end	Single end	Paired end	Single end
Read length	50	100	50	36	100	36
Total no. of reads	96,331,255	46,748,370	74,481,942	41,283,763	52,103,334	41,270,151
No. of mapped reads	92,513,698	41,423,212	70,860,588	39,989,804	36,610,869	35,340,075
Mapping (%)	96.04	88.61	95.13	96.87	70.27	85.63

tional studies today have focused only on a few laboratory strains, such as H99, it is critical to investigate the transcriptional responses of other wild-type strains (16).

The ability to investigate the genetic responses of a pathogenic microbe within its host offers a powerful opportunity to elucidate the adaptive strategies that are essential for the microbe to survive the hostile host environment. We propose that the gene expression profiles for yeasts in the host are both site and time specific. For instance, we hypothesize that human cryptococcal meningitis involves at least six stages: (i) initiation of infection in the lungs following the inhalation of yeasts or spores; (ii) yeast survival and proliferation within the lung; (iii) dormancy of yeast cells in the host tissue; (iv) reactivation of latent infection with renewed yeast growth; (v) dissemination of the yeasts via the blood, reticuloendothelial, and lymphatic systems, bridging the blood-brain barrier; and (vi) proliferation of yeasts in brain tissue and the subarachnoid space. At these various sites and durations of infection, the transcriptional responses of *C. neoformans* will vary in response to the unique host environment.

With this understanding, we have taken a very focused approach to identify regulated genes, networks, and signature markers that enable *C. neoformans* to survive and develop disease within the subarachnoid space. Using an experimental immunocompromised rabbit model of cryptococcal meningitis and the well-studied H99 strain of *C. neoformans*, we previously identified genes that were highly upregulated in the subarachnoid space of the CNS, such as isocitrate lyase (*ICL1*). Nevertheless, additional studies determined that despite its upregulation, *ICL1* was not essential for disease production at this site (17). Conversely, a gene in the trehalose pathway, the trehalose-6-phosphate synthase gene (*TPS1*), was also significantly upregulated in the CNS (18), and this pathway was shown to be critical for disease production (19, 20).

In this study, we examined and compared the cryptococcal transcriptome from two HIV-infected patients with high burdens of cryptococcal cells in the cerebrospinal fluid (CSF) at a single time point during infection. The patients resided in different geographical locations (Uganda and United States), and their strains represented the two global molecular types, VNI and VNII, of the dominant variety, *C. neoformans* var. *grubii*. We extracted RNA from the yeast cells taken directly from CSF and used Illumina-based RNA-seq technology to analyze their transcriptomes. These *in vivo* transcriptomes were compared with each other and with the transcriptomes of each strain after incubation in pooled human CSF (*ex vivo*) or *in vitro* growth in YPD broth. These conditions replicated simple exposure to CSF and late-logarithmic-phase growth in nutritionally replete medium.

RESULTS

Analysis of two clinical *C. neoformans* var. *grubii* isolates. Isolates of *C. neoformans* var. *grubii* were obtained from two untreated patients with cryptococcal infections and AIDS. Strain G0 was obtained from a patient in Uganda participating in the COAT trial (http://clinicaltrials.gov/ct2/show/nct01075152), and strain HC1 was isolated from a patient in the United States. Both strains possess the capsular A serotype and the α mating-type allele. Eight unlinked multilocus sequence typing (MLST) loci (21) were used to determine molecular genotypes of the two strains by comparison with 30 representative strains from the global population of *C. neoformans* (see Table S1 in the supplemental material). Previously, we demonstrated that the global population of *C. neoformans* var. *grubii* strains can be categorized within one of three genetically isolated subpopulations or molecular types, identified as VNI, VNII, and VNB (22). Maximum parsimony analysis determined that the G0 strain has molecular type VNI, and the HC1 strain is molecular type VNII (see Fig. S1) (16, 21, 22). More specifically, strain G0 has the same genotype as the globally prevalent reference VNI strain UG2471 (see Fig. S1) and the MLST-designated genotype M3b (see Table S1) (16). The MLST genotype of strain HC1 matches that of the VNII reference strain C45 (see Fig. S1), which was previously designated genotype M7c (see Table S1) (16). These two genotypes are globally distributed: other VNI isolates with the M3b genotype have been reported from clinical cases in Belgium, Brazil, Botswana, India, South Africa, and Uganda, and isolates of VNII with the M7c genotype have been found in South Africa and the United States (16, 21, 22).

Six cDNA libraries were created for high-throughput Illumina sequencing. Two libraries were made from yeast cells that were directly isolated from the two patients. The remaining four libraries were made from cultures obtained by inoculating the cryptococcal isolates in either YPD or *ex vivo* CSF (see Materials and Methods). In total, more than 350 million reads were generated, representing on average more than 100× coverage of the *C. neoformans* genome length for each sample (Table 1).

We aligned all the sequence reads to the *C. neoformans* var. *grubii* H99 genome using Bowtie (23) and TopHat (24). For most samples, more than 85% of the reads mapped to the genome, and there were no major differences among the RNA obtained from the patients' yeast cells (*in vivo* CSF) and the *in vitro* cultures incubated in CSF or YPD (Table 1). We measured the expression levels in fragments per kilobase of exon model per million mapped reads (FPKM) (25), and the gene expression level was defined as the sum of the FPKM values of its isoforms. Due to the high sensitivity of the RNA-seq technique, almost the entire gene set of the *C. neoformans* genome was detected as expressed (FPKM $\geq$ 1) under all three conditions. Of the 6,976 genes predicted by the

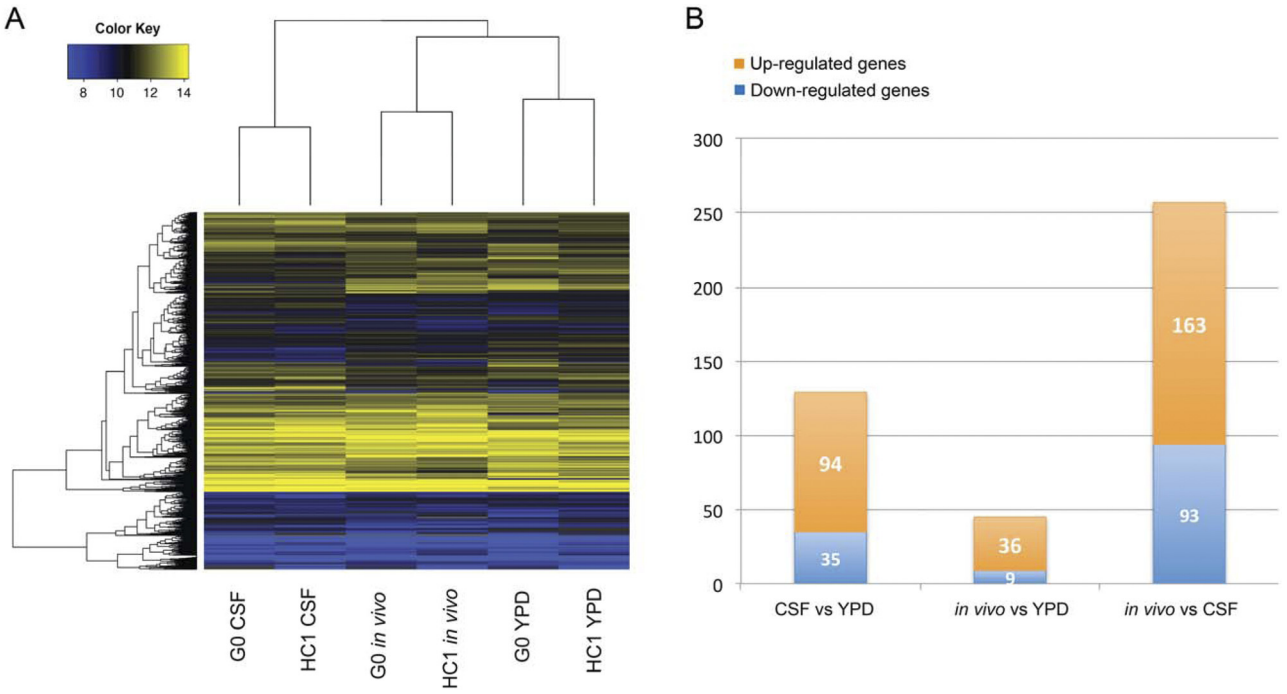

FIG 1 (A) Hierarchical cluster analysis of gene expression based on log ratio of normalized read count per gene. The cluster displays expression patterns for six RNA-seq samples. The color key represents $\log_2$-normalized transformed counts. (B) Number of genes that are significantly up/downregulated (FDR < 0.2) between two different conditions in both strains. Pairwise comparisons were made between three conditions: *ex vivo* CSF versus YPD, *in vivo* CSF versus YPD, and *in vivo* CSF versus *ex vivo* CSF. The numerical designation indicates the number of genes that were up/downregulated in the first condition compared to that in the second condition. See Table S2 in the supplemental material for a list of these genes.

H99 genome, 6,778 (97.16%), 6,647 (95.28%), and 6,809 (97.60%) genes were expressed in G0 under YPD, *ex vivo* CSF, and *in vivo* conditions, respectively, and in HC1, 6,849 (98.18%), 6,620 (94.89%), and 6,778 (97.16%) genes were expressed under the same three conditions. A total of 6,363 (91.21%) genes were expressed in both strains under all conditions. In contrast, 207 or 190 genes were exclusively expressed in either G0 or HC1, respectively, under one or more of the three conditions.

Analysis and evaluation of differential gene expression. In order to compare gene expression levels among different environmental conditions, we generated the whole gene expression profile using all the RNA-seq data by HT-Seq count (http://www-huber.embl.de/users/anders/HTSeq) and normalized using the DESeq package (26) in R (27). Hierarchical clustering indicated that the expression profiles of the two strains growing under the same conditions were more similar to each other than the patterns of transcription of each strain under different conditions (Fig. 1A). This similarity is notable because the duration of CNS infection with each strain was unknown but likely differed. In addition, strains G0 and HC1 represent divergent molecular types of *C. neoformans* var. *grubii*, VNI and VNII, respectively (22, 28, 29). These observations demonstrate the possibility that *in vivo* transcriptomes of additional strains might reveal more conserved *in vivo* genetic signatures.

Although serial *in vivo* CSF specimens were not available for our study, the similarity of gene expression patterns of the two strains under different conditions allowed us to regard the two strains under the same conditions as biological replicates. This approach allowed us to identify common transcriptional responses that are relevant for both genotypes. A modified Fisher's exact test with data fit to a negative binomial distribution of the DESeq package (26) was used to identify the differentially expressed (DE) genes. We made pairwise comparisons between different conditions, and the numbers of DE genes are as follows (Fig. 1B): *ex vivo* CSF versus YPD, 129 (see Table S2A); *in vivo* versus YPD, 45 (see Table S2B); *in vivo* versus *ex vivo* CSF, 256 (see Table S2C). These comparisons indicate that the transcriptional profiles of the *in vivo* CSF and YPD samples were actually more similar to each other than to *ex vivo* CSF samples. These results are also consistent with the hierarchical clustering of the transcriptional profiles in the dendrogram display (Fig. 1A). This finding might be explained by the potentially more active yeast cell growth in YPD and the host than is present during *ex vivo* CSF exposure. Gene ontology (GO) analysis was used to identify functional categories overrepresented in the DE genes. Compared to yeast cells that were incubated *ex vivo* in CSF, yeasts from *in vivo* CSF upregulated the expression of genes that were enriched in GO terms that related to cell metabolism, such as cellular biosynthetic processes (GO:0044249, $P = 1e{-}12$), gene expression (GO:0010467, $P = 5.4e{-}19$), and structural constituents of ribosome (GO:0003735, $P < 1e{-}30$). The increased expression of ribosomal protein genes indicated that the yeast cells were more biosynthetically active within the human brain and subarachnoid space, where they were confronted by host inflammatory cells and processes. Compared to nutrient-rich YPD, human (*in vivo* and *ex vivo*) CSF is a nutritionally depleted environment. We hypothesized that the genes upregulated in the CSF (*in vivo* or *ex vivo*) might be more related to biological survival and/or fitness of *C. neoformans* in the human subarachnoid space. Indeed, 20 genes were identified to be significantly upregulated in *in vivo* and *ex vivo* CSF conditions

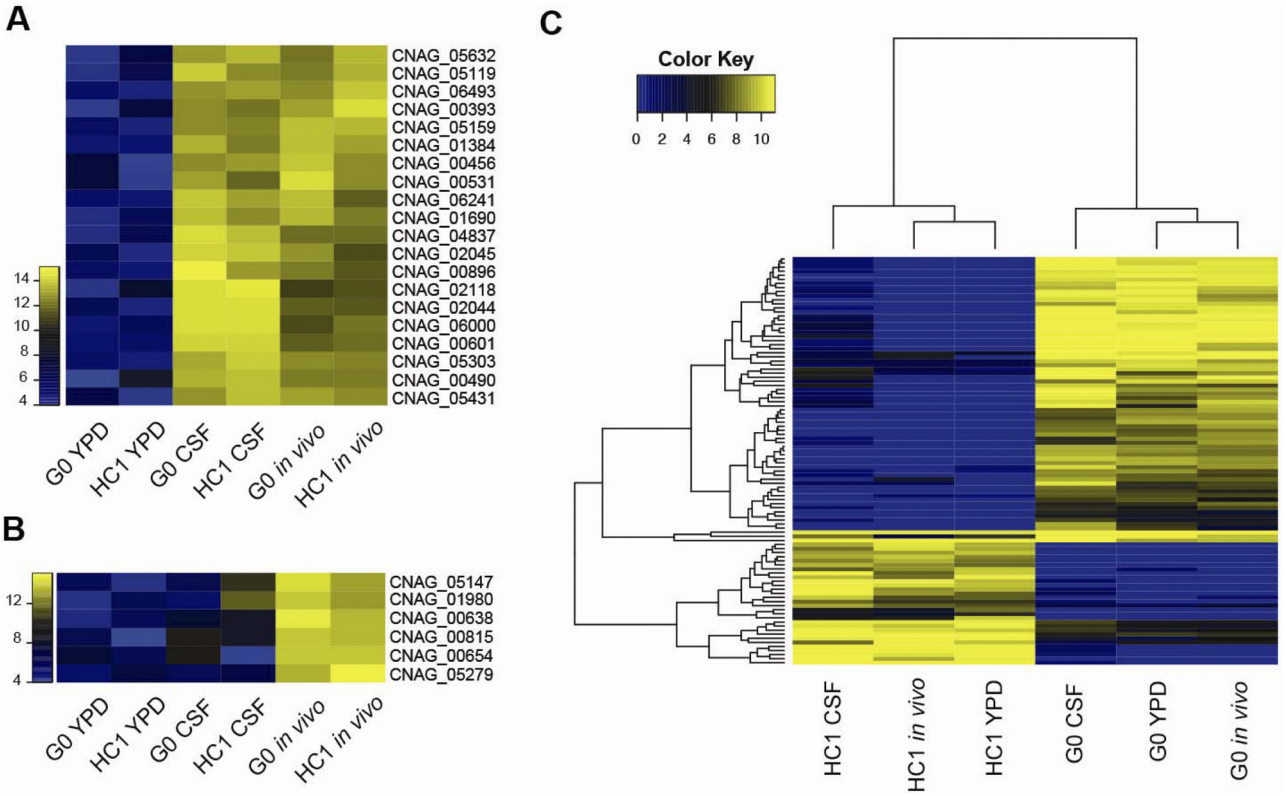

FIG 2 Heatmaps showing the expression data of 20 genes that were significantly upregulated in *ex vivo* CSF and *in vivo* CSF compared to YPD in both strains (A) and the expression data of six genes that were significantly upregulated in *in vivo* CSF compared to in *ex vivo* CSF and YPD in both strains (B). (C) Hierarchical cluster analysis of the 100 most divergently expressed genes between G0 and HC1.

compared with that in YPD (Fig. 2A; see also Table S3A in the supplemental material). As predicted, several of these identified genes have been reported as putative virulence or fitness genes in *C. neoformans*, such as *CFO1* (30), *ENA1* (31, 32), and *RIM101* (33). However, six of the 20 genes had no functional annotation; two of them (CNAG_00456 and CNAG_05159) were identified as the putative target genes of Gat201 (3), which is known as a regulator of virulence (34).

To analyze the specificity of the transcriptional responses of *C. neoformans* in the human body, six genes were significantly upregulated in the *in vivo* CSF compared to the other two conditions (Fig. 2B; see Table S3B in the supplemental material). Among these genes, the sulfiredoxin gene (*SRX1*) has been reported to have a critical role in the resistance of yeasts and higher eukaryotes to oxidative stress (35, 36). In addition, the high expression of *SRX1* might be critical for survival of the yeasts in the presence of monocytes/macrophages in CSF or microglial cells in brain parenchyma. Furthermore, another upregulated gene, *SIT1*, has been reported to be essential for growth, melanin formation, and cell wall density of *C. neoformans* under low-iron conditions (37) and for invasion of epithelial cells by *Candida albicans* (38). The expression of *SIT1* as well as *CFO1* indicates the potential importance of iron at this site.

To verify the potential relevance of genes that were shown by RNA-seq to be upregulated in CSF, four of the DE genes were selected for quantification of their expression by real-time reverse transcription-PCR (RT-PCR). Due to the low quantity of *in vivo* RNA sample of the G0 strain, cDNAs of five different samples were used as the templates. Transcription of *ACT1* was used to confirm and normalize the concentration of mRNA among different samples. The comparisons between RNA-seq and RT-PCR of these genes are shown in Fig. S2 in the supplemental material. Although some differences were shown in the HC1 YPD sample, most of the data were consistent between the two.

Strain-specific differentially expressed genes. As strains G0 and HC1 belonged to different genetic MLST subpopulations (see Table S1 and Fig. S1 in the supplemental material), we investigated their divergently expressed genes. A dissimilarity score was used to estimate the diversity of gene expression between the two strains. The 100 most divergently expressed genes were identified based on this dissimilarity score (Fig. 2C; see also Table S4). Based on the expression patterns, these genes can be organized into two groups: 69 genes (group 1) are expressed significantly more in G0 than in HC1 under all conditions, and 31 genes (group 2) are expressed significantly more in HC1 than in G0 under all conditions. Gene ontology analysis revealed that these 100 most divergently expressed genes evinced an enrichment for transporters ($P = 1.54e-4$).

Substantial genomic variation exists among G0, HC1, and H99. RNA-seq technology was developed primarily to analyze global gene expressions. However, the high coverage and good quality of the data provided us with an efficient way to assess the genetic diversity among clinical strains. Compared to the standard H99 clinical isolate from the United States, 50,155 single-nucleotide variants (SNVs) and 156,880 SNVs were identified in G0 and HC1, respectively (see Fig. S3 and Table S5 in the supple-

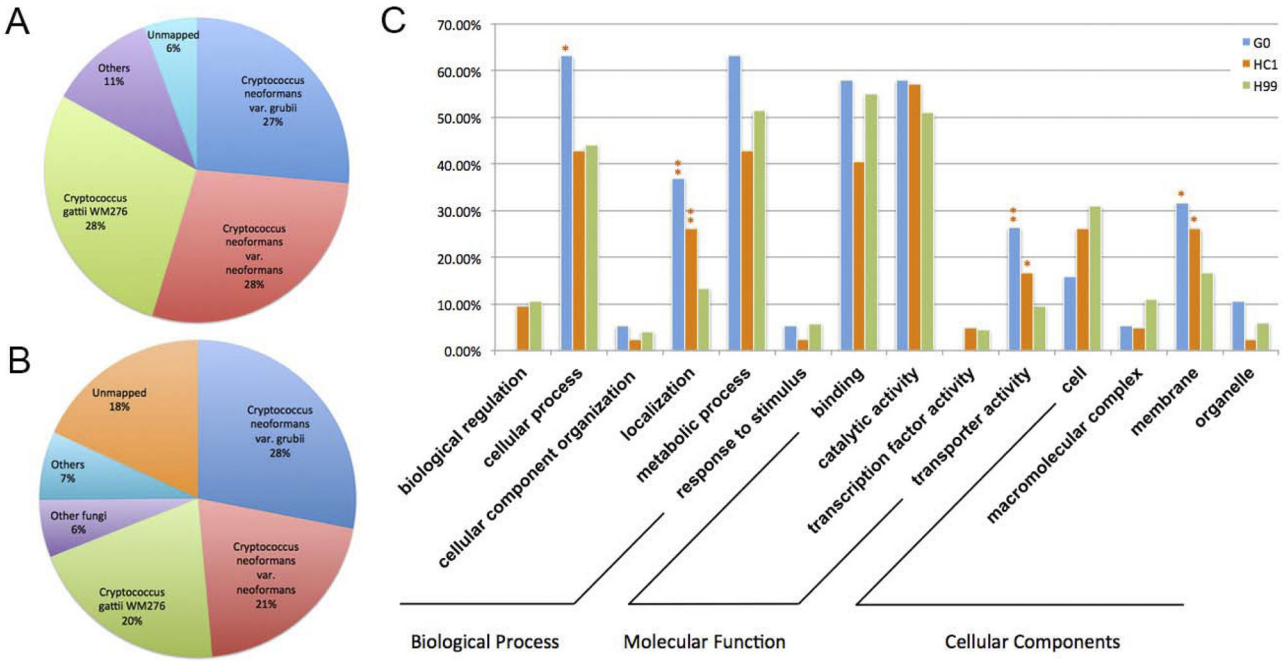

FIG 3 The proportions of the novel genes of G0 (A) and HC1 (B) that mapped to different species. (C) GO classification of novel genes of G0 and HC1 compared to those of H99. Percentages of genes annotated with certain GO terms compared to total number of annotated genes are shown in the figure. A hypergeometric test was used to test the enrichment of G0 and HC1 novel genes compared with H99 gene composition (*, $P < 0.05$; **, $P < 0.01$).

mental material). Strains H99 and G0 are prevalent VNI molecular types with respective MLST genotypes of M1b and M3b, and HC1 is a global VNII strain with the M7c genotype (see Table S1). In G0, 21,059 SNVs were dispersed in 5,185 genes, and in HC1, 104,027 SNVs were dispersed in 6,728 genes. The SNVs in the exon regions were further classified according to the open reading frame (ORF). In G0, 19,997 SNVs were detected in coding regions, of which 8,626 were nonsynonymous. In HC1, 99,542 SNVs were detected in coding regions, and 35,674 were nonsynonymous. The ORF regions contained 70 SNVs and 130 SNVs in G0 and HC1, respectively, which can cause changes between amino acids and stop codons. In these SNVs, 32 SNVs in G0 (see Table S6A) and 45 SNVs in HC1 were regarded as readthrough SNVs (see Table S6B), and the others were regarded as nonsense SNVs (see Table S6C and D). Due to changes in the stop codon, SNVs may affect protein translation and/or stability and cause phenotypic changes between the strains (39, 40). For example, one of the readthrough mutations has specifically occurred in G0 *OGG1* (CNAG_03795), which encodes a DNA glycosylase that is putatively involved in the repair of oxidative DNA damage (41). Therefore, in a phenotypic screen, we tested whether this gene variation had a phenotypic consequence on the three yeast strains. A higher level of resistance to H_2O_2 was observed in G0 than in H99 and HC1 (see Fig. S4). Although further studies will be required to determine whether this phenotypic change was specifically caused by this single nucleotide mutation, this observation underscores the ability to identify areas of potential genomic differences that translate into specific and sometimes subtle differences in cryptococcal strain phenotypes.

Gene gain and loss during evolution may also be critical for the functional differentiation between species and strains (42, 43). Therefore, to identify novel genes in both strains compared with a reference genome, we performed *de novo* assembly of the RNA-seq data using Trinity (44). A total of 18,260 and 24,664 contigs were assembled for G0 and HC1, respectively, which belonged to 8,996 and 10,268 unigenes (the nonredundant set of the contigs). We first aligned all the contigs against H99 genome and mitochondrial DNA sequences, but 53 unigenes in G0 and 171 unigenes of the more divergent HC1 could not be aligned to them. We then used BLAST to identify the homologs of these unaligned unigenes in the NCBI nonredundant nucleotide (nt) and nonredundant protein (nr) databases. Forty-four unigenes in G0 and 118 unigenes in HC1 were identified to homologous genes in the four fully sequenced *Cryptococcus* genomes (Fig. 3A and B). To investigate the putative functions of these novel genes, we used BLAST2GO (45) to annotate them. Nineteen genes in G0 and 42 genes in HC1 were assigned corresponding gene ontology terms, and they were enriched in functions related to transport, localization, and membrane constitution in both G0 and HC1 compared with the standard whole genome composition of H99 (Fig. 3C).

DISCUSSION

In this study, we generated genome-wide transcriptional profiles of *C. neoformans* var. *grubii* from two untreated AIDS patients. To our knowledge, this is the first report of RNA-seq data generated from yeast cells taken directly from human CSF. When we aligned the sequencing data to the reference genome of strain H99, the *in vivo* data from strain G0 received an extremely high ratio of hits (>95%), which indicated that RNA recovered from the *in vivo* samples was of high quality with very limited contamination. Analysis of *in vivo* transcription is especially challenging, because each *in vivo* sample is unique and cannot be duplicated, which is not ideal for applying classical strategies for quantitative analysis of transcriptional profiles (46, 47). To address this situation, we

treated the samples obtained from different patients as replicates in the analyses. The results demonstrated good reproducibility of the gene expression patterns between the two different clinical strains. Using this approach, we were able to compare and identify genes whose expression is associated with *in vivo* survival and growth. This strategy can be used in future analyses of *in vivo* samples.

To identify genes whose expression is associated with *in vivo* growth, we assessed transcriptional profiles of the two strains under two defined *in vitro* conditions, YPD and *ex vivo* CSF, and compared them with expression in the *in vivo* environment. We hypothesized that because of low nutrients in human CSF, the *in vivo* gene expression profile would be more similar to that observed in *ex vivo* CSF than YPD, which is nutritionally replete. This hypothesis was supported by our previous data that the ability of *C. neoformans* mutants to survive *in vitro* in human CSF was closely correlated with their production of disease in a rabbit meningitis model (48). Contrary to our expectations, in this study we observed that the *in vivo* gene expression profiles of *C. neoformans* strains in human CSF were generally more similar to those in YPD than to *ex vivo* CSF (Fig. 1). Gene ontology enrichment analysis revealed that the downregulated genes in *ex vivo* CSF samples compared to those in *in vivo* human samples were significantly enriched in metabolic and cellular processes. These results suggest that the yeast cells are inhibited in their basic metabolic machinery in the *ex vivo* CSF; however, inside the host (*in vivo* CSF), yeast cells maintain an active metabolic gene network and actively proliferate. The results are also consistent with the observations that during human disease, the number of yeast CFUs can increase to more than 1 million CFU/ml in an HIV-infected patient (49), and in the immunosuppressed rabbit model, abundant yeast growth occurs in the subarachnoid space (50). There are several nonexclusive explanations of why *C. neoformans* growth measured by viable quantitative yeast counts is inhibited in *ex vivo* CSF but active *in vivo*. First, in humans, CSF is constantly being renewed, and therefore *in vivo* CSF has a much higher concentration of nutrients than *ex vivo* CSF. Second, *ex vivo* CSF has a much more alkaline pH compared to that of *in vivo* CSF, which can affect transcription. Third, *C. neoformans* cells colonize human CNS after going through several stages of infection, which may extend for months or even years. This slow progression through the infection process can cause genetic and epigenetic adaptations and subsequent changes in the gene expression patterns, which are detectible in yeast cells obtained directly from humans but lost *in vitro* because the yeast cells exposed to *ex vivo* CSF were propagated in culture prior to CSF exposure.

Although the growth state of yeast cells in *ex vivo* CSF and human subarachnoid space (*in vivo*) may not be the same, there are stresses from this specific fluid environment that are similar and unique. Therefore, the 20 genes that we identified as significantly upregulated in the two CSF conditions compared to YPD might specifically represent the response of *C. neoformans* to certain CSF stresses or signals. Based on the annotation information in FungiDB (51), most of these genes are categorized into three groups: catalytic activity-related genes (6/20), transporters (5/20), and genes of unknown function (6/20). Two of these genes have been reported as necessary survival genes for *C. neoformans*. We previously demonstrated that the ATPase transporter gene *ENA1* is essential for survival of this yeast in CSF (48). Jung et al. showed that the ferroxidase, *CFO1*, is required for the utilization of the biological protein, transferrin, which is an important iron source for *C. neoformans* during infection (30). We did not observe any evidence for differential regulation of any of the classical virulence factors (capsule, melanin, high-temperature growth, urease, phospholipase) at this advanced clinical state of infection, most likely because these classical virulence factors are expressed during the early stages of infection in the lungs and/or during dissemination. Conversely, our data suggest that basic metabolic pathways and stress response genes are essential for survival and successful propagation within the subarachnoid space.

As we investigate *in vivo* gene expression data between humans and animal models and compare those with the data obtained for other fungal infections, it is possible to recognize conserved patterns of gene regulation. For example, the isocitrate lyase gene (*ICL1*) and the glyoxylate pathway are upregulated in both human and experimental animal models of cryptococcal meningitis. In addition, recent work by Cheng et al. demonstrated the upregulation of *RIM101* in peritoneal *Candida* infections in mice (52), which is similar to our observation of CNS infection with *Cryptococcus* in humans. With the analyses of further cases, we expect to find common conserved pathways that are characteristic for development of the disease.

To investigate the six differentially regulated genes with unknown functions, we searched the annotated fungal genomes available in FungiDB and found that four of them (CNAG_02118, CNAG_04837, CNAG_05632, and CNAG_06493) are restricted to *Cryptococcus* lineage. Such lineage-specific genes are often important for species evolution. For example, it has been demonstrated that in primates, lineage-specific genes are essential for human brain evolution (53). We hypothesize that in *Cryptococcus*, lineage-specific genes may be important for adaptation of *Cryptococcus* in its survival within certain human body sites. More studies are required to test this hypothesis, and we have now begun to identify the genes of interest.

Transporters are groups of genes that play important roles in yeast biology. In our study, transporter genes were frequently identified in many different analyses. Based on our results, we divided the transporter genes into two groups. One group includes the transporters that are conserved among different strains or even distantly related species, and they are essential for *Cryptococcus*. Several of these transporters have been identified and studied previously (54–57). Three genes from this group of transporters with previously defined function, *CFO1*, *ENA1*, and *SIT1*, were significantly upregulated in both *in vivo* and *ex vivo* CSF compared to in YPD. These genes are important for virulence, drug resistance, starvation response, intracellular survival, and other basic functions in *Cryptococcus* (30, 31, 37, 48, 58). The second group of transporters includes rapidly evolving and variable genes that may not be particularly essential for the yeast's pathobiology. These transporters have different expression patterns or even different genetic compositions among genetically related strains. In our study, these transporter genes were enriched among the most divergently expressed and novel genes. Most of these genes have been annotated as carbohydrate transporters, such as a sugar transporter, monosaccharide transporter, galactose transporter, and hexose transporter. Although the exact function of these transporters is unknown, they might be involved in the biosynthesis of the polysaccharide capsule of *Cryptococcus*, which is one of its main virulence factors (59). In addition to carbohydrate transporters, we also observed several novel genes that belonged to the

major facilitator superfamily (MFS) transporters and ATP-binding cassette (ABC) transporters, which have been shown to play a role in multidrug resistance of fungi (60). We hypothesize that this group of transporters may contribute to variable strain-specific properties and even explain the differences in disease manifestations and treatment outcomes between strains. Indeed, when the two strains were compared for the most divergently expressed genes, transporter genes were commonly identified, and these findings support the hypothesis that the microevolution of these strain-specific properties frequently involves transporter functions. However, more studies are necessary to evaluate the potential role of the second group of transporters in the pathogenesis of *C. neoformans* and how genetic changes in these transporters influence a strain's unique phenotype.

This first analysis of cryptococcal transcriptomes during infection in the CNS has demonstrated a series of important principles. First, the transcriptomes of cryptococcal cells from the human host can be captured and analyzed. Second, despite genetic differences between strains and the duration of their infection, the transcriptomes from these strains are remarkably similar and suggest that a specific consensus pattern of gene expression may be associated with CNS infection. Third, *C. neoformans* is metabolically active in the human CSF. Fourth, specific genes with known virulence or survival properties are identified using *in vivo* transcription profiling, which validates this method. Moreover, genes and pathways essential for survival of yeasts in the human body are not limited to classical virulence pathways or phenotypes. Fifth, through the combination of RNA-seq and genome analysis, identification of SNVs and other genetic diversities may predict differences in gene expression and/or function in individual strains and identify the potential impact of these mutations on yeast microevolution. Additional strategies are needed to determine the functions of nonconserved genes that lack homology to annotated sequences, as they may be essential for the pathogenicity of *C. neoformans*. Comparative analyses of transcriptomes may identify the potential importance of these unrecognized genes. This study is just the beginning, but it illustrates the potential to characterize fungal transcriptomes and then relate them to the progressive states of disease. They may provide insights into how a strain(s) produces disease and how some strains might produce a genetic signature that could even predict their infection outcome or response to therapy.

MATERIALS AND METHODS

DNA manipulations and phylogenetic analyses. Genomic DNA was isolated using a MasterPure yeast DNA purification kit (Epicentre Biotechnologies, Madison, WI). As previously described, mating types were determined by a PCR-based method using primers for the **a** or α allele of the STE20 gene for the strains (61). For MLST, eight previously described loci (*CAP59*, *GPD1*, *IGS1*, *LAC1*, *PLB1*, *SOD1*, *URA5*, and *TEF1*) were used in this study for PCR amplification (22, 62). Amplicons were sequenced with Sanger sequencing, and the reads were edited manually. To identify the genotypes of G0 and HC1, their MLST sequences were compared with a global set of reference strains of *C. neoformans* (see Table S1). The sequences of all the loci were aligned by ClustalW (63). The maximum parsimony (MP) tree was identified with heuristic searches based on 500 random sequence additions using PAUP (64) and was rooted using *C. neoformans* strain JEC21 (serotype D).

RNA-seq sample preparation. Yeast cells (approximately 10^6 to 10^8 CFUs) were pelleted in CSF in a microfuge tube containing 20 to 30 μl of 1-mm glass beads, and the pellet was stored at −80°C. The frozen pellet was lyophilized and vortexed to powder, and RNA was extracted using a modified Trizol/Qiagen procedure as follows: yeast cells were lysed in 700 μl Trizol and incubated for 5 min at room temperature. After 140 μl of chloroform was added, the tube was shaken for 20 s and incubated at room temperature for 3 min. The sample was centrifuged at 10,000 rpm for 15 min at room temperature. The aqueous phase was separated and mixed with equal volumes of 80% ethanol and immediately applied to a Qiagen RNeasy minicolumn (Qiagen; catalog number 74014) and centrifuged at 13,000 rpm for 1 min, and RNA was isolated according to the manufacturer's protocol. The yield of total RNA ranged between 1 and 25 mg/ml.

The CSF samples were part of the Duke IRB-approved database and Specimen Repository for Infectious Disease Related Studies (PR0005314) in which patients are deidentified and clinical information is limited. The HC1 strain came from a patient in the United States, and strain G0 was from a Uganda patient. YPD broth (1% yeast extract, 1% Bacto peptone, 2% dextrose) and sterile human CSF (pool of 10 to 20 individuals) were prepared as previously described (48) and used for *in vitro* or *ex vivo* incubation of the strains. The strains were grown in YPD broth for 16 h at 37°C and then harvested. Yeast cells in stationary phase after culture in YPD overnight at 37°C were exposed to human CSF for 9 h, during which the CSF was replenished every 3 h, and the cells were then harvested. All harvested cells were snap-frozen and lyophilized for total RNA isolation.

RNA sequencing and quantitative analysis. Total RNAs from the two strains (HC1 and G0) under the various conditions were extracted using Trizol (Invitrogen) according to the manufacturer's instructions. The mRNA samples for RNA-seq analysis were performed using a TruSeq RNA sample preparation kit (Illumina, San Diego, CA). The cDNA libraries were sequenced on the Illumina GAII and the Illumina HiSeq 2000 (Illumina, San Diego, CA) instruments. The *C. neoformans* var. *grubii* H99 genome with annotations (2012 release) were downloaded from the Broad Institute (http://www.broadinstitute.org) and used as a reference. Sequencing reads of each sample were mapped to a reference genome using TopHat 2.0.0 (24). Subsequently, we used the HT-Seq count (http://www-huber.embl.de/users/anders/HTSeq) to convert the mapped reads to read counts per gene. In the quantitative analysis, the two isolates exposed to the same conditions were treated as biological duplicates. We evaluated the expression differences using a test based on a negative binomial distribution, which was implemented in the R package DESeq (26). Three comparisons were made among the different conditions: (i) *in vivo* human versus YPD; (ii) *in vivo* CSF versus *ex vivo* CSF exposed; (iii) *ex vivo* CSF exposed versus YPD. The false discovery rate (FDR) was calculated by the "p.adjust" function in R using the Benjamini and Hochberg (65) method and controlled at 20%. All selected FDR-adjusted *P* values corresponded to raw *P* values below 0.01. The number of fragments per kilobase of exon model per million mapped reads (FPKM) was calculated according to Cufflinks (25). A dissimilarity score was defined as follows:

$$\text{dissimilarity score} = 1 - \Sigma_i \frac{2P_i(\text{A})P_i(\text{B})}{P_i^2(\text{A}) + P_i^2(\text{B})}$$

where $P_i(\text{A})$ and $P_i(\text{B})$ represent the normalized expression value of gene *i* in strain A and strain B under the same condition.

Quantitative real-time RT-PCR validation of RNA-seq data. Total RNA of each sample was treated with DNase (Turbo DNA-free kit; Ambion) to avoid genomic DNA contamination. Reverse transcription was performed using the RETROscript kit (Ambion). Four genes were selected for validation of RNA-seq results using RT-PCR. Primer pairs were designed to span exon-exon junctions using Primer3, and *ACT1* was used as an internal control. All the primer sequences are as follows (5′ to 3′): *ACT1*, CCACACTGTCCCCATTTACGA (forward) and CAGCAAGATC GATACGGAGGAT (reverse); CNAG_05431, AAGCCCCCTGAGAGAC CTAG (forward) and GGAGCTCCAACAGACTCGA (reverse); CNAG_06493, AACAGACGGCATCGAAGGTT (forward) and GTTAC AGAATGCTGCGCTCG (reverse); CNAG_00654, TGTCAGAACCAGC ATGAGGC (forward) and CCGCCCTACCTTCCGTAATC (reverse); CNAG_00815, ACCTGGCATCGATGGGTTTT (forward) and TGGAG

GTTGCGGTCACAATA (reverse). The amplifications were conducted in a total volume of 20 μl, containing 1× SYBR green (iTaq universal SYBR green supermix; Bio-Rad), 300 nmol/liter of both primers, and 1 μl of diluted cDNA. The amplification was conducted as follows: 5 min at 95°C, followed by 35 cycles consisting of 30 s at 95°C, 30 s at 54°C, and 30 s at 72°C. Finally, melting curve analysis was performed from 60°C to 95°C, with increments of 0.5°C per 10 s. Amplification, melting curve analysis, and detection were conducted with the MyiQ single-color, real-time PCR detection system (Bio-Rad).

RNA-seq variant calling. BAM files that were generated by TopHat were used as inputs. The genome analysis toolkit (GATK version 2.4.9) (66) was used to perform variant calling. To solve the incompatible scores between TopHat and GATK, all the mapping scores with 255 in TopHat were reassigned to 60 in GATK. The filter used in GATK was "-stand_callconf 50 -stand_emitconf 10 -dcov 500." All the SNVs were annotated using VCFannotator (http://vcfannotator.sourceforge.net) relative to the H99 genome.

Detection and characterization of novel genes. To obtain high-quality assemblies for the transcriptomes, we used only 100-bp paired-end reads for *de novo* assembly. Reads that contained more than 10% of the bases with phred quality scores below 20 were removed using FASTX toolkit (http://hannonlab.cshl.edu/fastx_toolkit). *De novo* assembly of the filtered reads was performed by Trinity (44). To detect the unigenes that either do not exist or were highly divergent from the reference genome, we aligned all the contigs to the *C. neoformans* var. *grubii* H99 genome and the mitochondrial DNA sequence using BLAT (67). A novel gene was defined as one for which all the contigs could not be aligned to the reference sequences. All the unigenes that met this criterion were aligned to the NCBI nonredundant nucleotide (nt) and protein database (nr) using BLAST. All the BLAST hits with *E* values less than 1e−5 were kept for further analysis.

RNA-seq data accession number. RNA-seq data have been made publicly available at GEO (http://www.ncbi.nlm.nih.gov/geo) under accession number GSE51573.

SUPPLEMENTAL MATERIAL

Supplemental material for this article may be found at http://mbio.asm.org/lookup/suppl/doi:10.1128/mBio.01087-13/-/DCSupplemental.

Table S1, PDF file, 0.1 MB.
Table S2, XLS file, 0.1 MB.
Table S3, PDF file, 0.1 MB.
Table S4, XLS file, 0.1 MB.
Table S5, PDF file, 0.1 MB.
Table S6, XLS file, 0.1 MB.
Figure S1, TIF file, 0.1 MB.
Figure S2, TIF file, 0.1 MB.
Figure S3, TIF file, 0.5 MB.
Figure S4, TIF file, 0.2 MB.

ACKNOWLEDGMENTS

This work was generously supported by Public Service grant AI7386 and AI93257 (J.R.P.).

The use of product names in this article does not imply their endorsement by the U.S. Department of Health and Human Services. The finding and conclusions in this article are those of the authors and do not necessarily represent the views of CDC.

REFERENCES

1. **Park BJ, Wannemuehler KA, Marston BJ, Govender N, Pappas PG, Chiller TM.** 2009. Estimation of the current global burden of cryptococcal meningitis among persons living with HIV/AIDS. AIDS **23:**525–530. http://dx.doi.org/10.1097/QAD.0b013e328322ffac.
2. **Heitman J.** 2011. Cryptococcus: from human pathogen to model yeast. American Society for Microbiology, Washington, DC.
3. **Chun CD, Brown JC, Madhani HD.** 2011. A major role for capsule-independent phagocytosis-inhibitory mechanisms in mammalian infection by *Cryptococcus neoformans*. Cell Host Microbe **9:**243–251. http://dx.doi.org/10.1016/j.chom.2011.02.003.
4. **Ngamskulrungroj P, Price J, Sorrell T, Perfect JR, Meyer W.** 2011. *Cryptococcus gattii* virulence composite: candidate genes revealed by microarray analysis of high and less virulent Vancouver Island outbreak strains. PLoS One **6:**e16076. http://dx.doi.org/10.1371/journal.pone.0016076.
5. **Kmetzsch L, Staats CC, Simon E, Fonseca FL, Oliveira DL, Joffe LS, Rodrigues J, Lourenço RF, Gomes SL, Nimrichter L, Rodrigues ML, Schrank A, Vainstein MH.** 2011. The GATA-type transcriptional activator Gat1 regulates nitrogen uptake and metabolism in the human pathogen *Cryptococcus neoformans*. Fungal Genet. Biol. **48:**192–199. http://dx.doi.org/10.1016/j.fgb.2010.07.011.
6. **Kronstad J, Saikia S, Nielson ED, Kretschmer M, Jung W, Hu G, Geddes JM, Griffiths EJ, Choi J, Cadieux B, Caza M, Attarian R.** 2012. Adaptation of *Cryptococcus neoformans* to mammalian hosts: integrated regulation of metabolism and virulence. Eukaryot. Cell **11:**109–118. http://dx.doi.org/10.1128/EC.05273-11.
7. **Chaturvedi V, Nierman WC.** 2012. *Cryptococcus gattii* comparative genomics and transcriptomics: a NIH/NIAID white paper. Mycopathologia **173:**367–373. http://dx.doi.org/10.1007/s11046-011-9512-9.
8. **Kraus PR, Boily MJ, Giles SS, Stajich JE, Allen A, Cox GM, Dietrich FS, Perfect JR, Heitman J.** 2004. Identification of *Cryptococcus neoformans* temperature-regulated genes with a genomic-DNA microarray. Eukaryot. Cell **3:**1249–1260. http://dx.doi.org/10.1128/EC.3.5.1249-1260.2004.
9. **Chow ED, Liu OW, O'Brien S, Madhani HD.** 2007. Exploration of whole-genome responses of the human AIDS-associated yeast pathogen *Cryptococcus neoformans* var. *grubii*: nitric oxide stress and body temperature. Curr. Genet. **52:**137–148. http://dx.doi.org/10.1007/s00294-007-0147-9.
10. **Jung WH, Saikia S, Hu G, Wang J, Fung CK, D'Souza C, White R, Kronstad JW.** 2010. HapX positively and negatively regulates the transcriptional response to iron deprivation in *Cryptococcus neoformans*. PLoS Pathog. **6:**e1001209. http://dx.doi.org/10.1371/journal.ppat.1001209.
11. **Haynes BC, Skowyra ML, Spencer SJ, Gish SR, Williams M, Held EP, Brent MR, Doering TL.** 2011. Toward an integrated model of capsule regulation in *Cryptococcus neoformans*. PLoS Pathog. **7:**e1002411. http://dx.doi.org/10.1371/journal.ppat.1002411.
12. **Pukkila-Worley R, Gerrald QD, Kraus PR, Boily MJ, Davis MJ, Giles SS, Cox GM, Heitman J, Alspaugh JA.** 2005. Transcriptional network of multiple capsule and melanin genes governed by the *Cryptococcus neoformans* cyclic AMP cascade. Eukaryot. Cell **4:**190–201. http://dx.doi.org/10.1128/EC.4.1.190-201.2005.
13. **Song MH, Lee JW, Kim MS, Yoon JK, White TC, Floyd A, Heitman J, Strain AK, Nielsen JN, Nielsen K, Bahn YS.** 2012. A flucytosine-responsive Mbp1/Swi4-like protein, Mbs1, plays pleiotropic roles in antifungal drug resistance, stress response, and virulence of *Cryptococcus neoformans*. Eukaryot. Cell **11:**53–67.
14. **Fan W, Kraus PR, Boily MJ, Heitman J.** 2005. *Cryptococcus neoformans* gene expression during murine macrophage infection. Eukaryot. Cell **4:**1420–1433. http://dx.doi.org/10.1128/EC.4.8.1420-1433.2005.
15. **Hu G, Cheng PY, Sham A, Perfect JR, Kronstad JW.** 2008. Metabolic adaptation in *Cryptococcus neoformans* during early murine pulmonary infection. Mol. Microbiol. **69:**1456–1475. http://dx.doi.org/10.1111/j.1365-2958.2008.06374.x.
16. **Litvintseva AP, Mitchell TG.** 2012. Population genetic analyses reveal the African origin and strain variation of *Cryptococcus neoformans* var. *grubii*. PLoS Pathog. **8:**e1002495. http://dx.doi.org/10.1371/journal.ppat.1002495.
17. **Rude TH, Toffaletti DL, Cox GM, Perfect JR.** 2002. Relationship of the glyoxylate pathway to the pathogenesis of *Cryptococcus neoformans*. Infect. Immun. **70:**5684–5694. http://dx.doi.org/10.1128/IAI.70.10.5684-5694.2002.
18. **Steen BR, Zuyderduyn S, Toffaletti DL, Marra M, Jones SJ, Perfect JR, Kronstad J.** 2003. *Cryptococcus neoformans* gene expression during experimental cryptococcal meningitis. Eukaryot. Cell **2:**1336–1349. http://dx.doi.org/10.1128/EC.2.6.1336-1349.2003.
19. **Ngamskulrungroj P, Gilgado F, Faganello J, Litvintseva AP, Leal AL, Tsui KM, Mitchell TG, Vainstein MH, Meyer W.** 2009. Genetic diversity of the *Cryptococcus* species complex suggests that *Cryptococcus gattii* deserves to have varieties. PLoS One **4:**e5862. http://dx.doi.org/10.1371/journal.pone.0005862.
20. **Petzold EW, Himmelreich U, Mylonakis E, Rude T, Toffaletti D, Cox**

GM, Miller JL, Perfect JR. 2006. Characterization and regulation of the trehalose synthesis pathway and its importance in the pathogenicity of *Cryptococcus neoformans*. Infect. Immun. **74:**5877–5887. http://dx.doi.org/10.1128/IAI.00624-06.
21. **Litvintseva AP, Carbone I, Rossouw J, Thakur R, Govender NP, Mitchell TG.** 2011. Evidence that the human pathogenic fungus *Cryptococcus neoformans* var. *grubii* may have evolved in Africa. PLoS One **6:**e19688. http://dx.doi.org/10.1371/journal.pone.0019688.
22. **Litvintseva AP, Thakur R, Vilgalys R, Mitchell TG.** 2006. Multilocus sequence typing reveals three genetic subpopulations of *Cryptococcus neoformans* var. *grubii* (serotype A), including a unique population in Botswana. Genetics **172:**2223–2238.
23. **Langmead B, Trapnell C, Pop M, Salzberg SL.** 2009. Ultrafast and memory-efficient alignment of short DNA sequences to the human genome. Genome Biol. **10:**R25. http://dx.doi.org/10.1186/gb-2009-10-3-r25.
24. **Trapnell C, Pachter L, Salzberg SL.** 2009. TopHat: discovering splice junctions with RNA-Seq. Bioinformatics **25:**1105–1111. http://dx.doi.org/10.1093/bioinformatics/btp120.
25. **Trapnell C, Williams BA, Pertea G, Mortazavi A, Kwan G, van Baren MJ, Salzberg SL, Wold BJ, Pachter L.** 2010. Transcript assembly and quantification by RNA-Seq reveals unannotated transcripts and isoform switching during cell differentiation. Nat. Biotechnol. **28:**511–515. http://dx.doi.org/10.1038/nbt.1621.
26. **Anders S, Huber W.** 2010. Differential expression analysis for sequence count data. Genome Biol. **11:**R106. http://dx.doi.org/10.1186/gb-2010-11-10-r106.
27. **Team RDC.** 2008. R: a language and environment for statistical computing. R Foundation for Statistical Computing, Vienna, Austria.
28. **Bovers M, Hagen F, Kuramae EE, Boekhout T.** 2008. Six monophyletic lineages identified within *Cryptococcus neoformans* and *Cryptococcus gattii* by multi-locus sequence typing. Fungal Genet. Biol. **45:**400–421. http://dx.doi.org/10.1016/j.fgb.2007.12.004.
29. **Meyer W, Castañeda A, Jackson S, Huynh M, Castañeda E, IberoAmerican Cryptococcal Study Group.** 2003. Molecular typing of IberoAmerican *Cryptococcus* neoformans isolates. Emerg. Infect. Dis. **9:**189–195.
30. **Jung WH, Hu G, Kuo W, Kronstad JW.** 2009. Role of ferroxidases in iron uptake and virulence of *Cryptococcus neoformans*. Eukaryot. Cell **8:**1511–1520. http://dx.doi.org/10.1128/EC.00166-09.
31. **Idnurm A, Walton FJ, Floyd A, Reedy JL, Heitman J.** 2009. Identification of ENA1 as a virulence gene of the human pathogenic fungus *Cryptococcus neoformans* through signature-tagged insertional mutagenesis. Eukaryot. Cell **8:**315–326. http://dx.doi.org/10.1128/EC.00375-08.
32. **Jang HH, Lee KO, Chi YH, Jung BG, Park SK, Park JH, Lee JR, Lee SS, Moon JC, Yun JW, Choi YO, Kim WY, Kang JS, Cheong GW, Yun DJ, Rhee SG, Cho MJ, Lee SY.** 2004. Two enzymes in one; two yeast peroxiredoxins display oxidative stress-dependent switching from a peroxidase to a molecular chaperone function. Cell **117:**625–635. http://dx.doi.org/10.1016/j.cell.2004.05.002.
33. **O'Meara TR, Norton D, Price MS, Hay C, Clements MF, Nichols CB, Alspaugh JA.** 2010. Interaction of *Cryptococcus neoformans* Rim101 and protein kinase A regulates capsule. PLoS Pathog. **6:**e1000776. http://dx.doi.org/10.1371/journal.ppat.1000776.
34. **Liu OW, Chun CD, Chow ED, Chen C, Madhani HD, Noble SM.** 2008. Systematic genetic analysis of virulence in the human fungal pathogen *Cryptococcus neoformans*. Cell **135:**174–188. http://dx.doi.org/10.1016/j.cell.2008.07.046.
35. **Soriano FX, Baxter P, Murray LM, Sporn MB, Gillingwater TH, Hardingham GE.** 2009. Transcriptional regulation of the AP-1 and Nrf2 target gene sulfiredoxin. Mol. Cells **27:**279–282. http://dx.doi.org/10.1007/s10059-009-0050-y.
36. **Biteau B, Labarre J, Toledano MB.** 2003. ATP-dependent reduction of cysteine–sulphinic acid by *S. cerevisiae* sulphiredoxin. Nature **425:**980–984. http://dx.doi.org/10.1038/nature02075.
37. **Tangen KL, Jung WH, Sham AP, Lian T, Kronstad JW.** 2007. The iron- and cAMP-regulated gene SIT1 influences ferrioxamine B utilization, melanization and cell wall structure in *Cryptococcus neoformans*. Microbiology **153:**29–41.
38. **Heymann P, Gerads M, Schaller M, Dromer F, Winkelmann G, Ernst JF.** 2002. The siderophore iron transporter of *Candida albicans* (Sit1p/Arn1p) mediates uptake of ferrichrome-type siderophores and is required for epithelial invasion. Infect. Immun. **70:**5246–5255. http://dx.doi.org/10.1128/IAI.70.9.5246-5255.2002.
39. **Yang P, Yang C, Wirschell M, Davis S.** 2009. Novel LC8 mutations have disparate effects on the assembly and stability of flagellar complexes. J. Biol. Chem. **284:**31412–31421. http://dx.doi.org/10.1074/jbc.M109.050666.
40. **Florent M, Noël T, Ruprich-Robert G, Da Silva B, Fitton-Ouhabi V, Chastin C, Papon N, Chapeland-Leclerc F.** 2009. Nonsense and missense mutations in FCY2 and FCY1 genes are responsible for flucytosine resistance and flucytosine-fluconazole cross-resistance in clinical isolates of *Candida lusitaniae*. Antimicrob. Agents Chemother. **53:**2982–2990. http://dx.doi.org/10.1128/AAC.00880-08.
41. **Arai K, Morishita K, Shinmura K, Kohno T, Kim SR, Nohmi T, Taniwaki M, Ohwada S, Yokota J.** 1997. Cloning of a human homolog of the yeast OGG1 gene that is involved in the repair of oxidative DNA damage. Oncogene **14:**2857–2861. http://dx.doi.org/10.1038/sj.onc.1201139.
42. **Dujon B, Sherman D, Fischer G, Durrens P, Casaregola S, Lafontaine I, de Montigny J, Marck C, Neuvéglise C, Talla E, Goffard N, Frangeul L, Aigle M, Anthouard V, Babour A, Barbe V, Barnay S, Blanchin S, Beckerich JM, Beyne E, Bleykasten C, Boisramé A, Boyer J, Cattolico L, Confanioleri F, de Daruvar A, Despons L, Fabre E, Fairhead C, Ferry-Dumazet H, Groppi A, Hantraye F, Hennequin C, Jauniaux N, Joyet P, Kachouri R, Kerrest A, Koszul R, Lemaire M, Lesur I, Ma L, Muller H, Nicaud J-M, Nikolski M, Oztas S, Ozier-Kalogeropoulos O, Pellenz S, Potier S, Richard G-F, Straub M-L, Suleau A, Swennen D, Tekaia F, Wésolowski-Louvel M, Westhof E, Wirth B, Zeniou-Meyer M, Zivanovic I, Bolotin-Fukuhara M, Thierry A, Bouchier C, Caudron B, Scarpelli C, Gaillardin C, Weissenbach J, Wincker P, Souciet J-L.** 2004. Genome evolution in yeasts. Nature **430:**35–44. http://dx.doi.org/10.1038/nature02579.
43. **Kemen E, Gardiner A, Schultz-Larsen T, Kemen AC, Balmuth AL, Robert-Seilaniantz A, Bailey K, Holub E, Studholme DJ, MacLean D, Jones JD.** 2011. Gene gain and loss during evolution of obligate parasitism in the white rust pathogen of *Arabidopsis thaliana*. PLOS Biol. **9:**e1001094. http://dx.doi.org/10.1371/journal.pbio.1001094.
44. **Grabherr MG, Haas BJ, Yassour M, Levin JZ, Thompson DA, Amit I, Adiconis X, Fan L, Raychowdhury R, Zeng Q, Chen Z, Mauceli E, Hacohen N, Gnirke A, Rhind N, di Palma F, Birren BW, Nusbaum C, Lindblad-Toh K, Friedman N, Regev A.** 2011. Full-length transcriptome assembly from RNA-Seq data without a reference genome. Nat. Biotechnol. **29:**644–652. http://dx.doi.org/10.1038/nbt.1883.
45. **Conesa A, Götz S, García-Gómez JM, Terol J, Talón M, Robles M.** 2005. Blast2GO: a universal tool for annotation, visualization and analysis in functional genomics research. Bioinformatics **21:**3674–3676. http://dx.doi.org/10.1093/bioinformatics/bti610.
46. **Nookaew I, Papini M, Pornputtapong N, Scalcinati G, Fagerberg L, Uhlén M, Nielsen J.** 2012. A comprehensive comparison of RNA-Seq-based transcriptome analysis from reads to differential gene expression and cross-comparison with microarrays: a case study in *Saccharomyces cerevisiae*. Nucleic Acids Res. **40:**10084–10097. http://dx.doi.org/10.1093/nar/gks804.
47. **Marioni JC, Mason CE, Mane SM, Stephens M, Gilad Y.** 2008. RNA-seq: an assessment of technical reproducibility and comparison with gene expression arrays. Genome Res. **18:**1509–1517. http://dx.doi.org/10.1101/gr.079558.108.
48. **Lee A, Toffaletti DL, Tenor J, Soderblom EJ, Thompson JW, Moseley MA, Price M, Perfect JR.** 2010. Survival defects of *Cryptococcus neoformans* mutants exposed to human cerebrospinal fluid result in attenuated virulence in an experimental model of meningitis. Infect. Immun. **78:**4213–4225. http://dx.doi.org/10.1128/IAI.00551-10.
49. **Bicanic T, Muzoora C, Brouwer AE, Meintjes G, Longley N, Taseera K, Rebe K, Loyse A, Jarvis J, Bekker LG, Wood R, Limmathurotsakul D, Chierakul W, Stepniewska K, White NJ, Jaffar S, Harrison TS.** 2009. Independent association between rate of clearance of infection and clinical outcome of HIV-associated cryptococcal meningitis: analysis of a combined cohort of 262 patients. Clin. Infect. Dis. **49:**702–709. http://dx.doi.org/10.1086/604716.
50. **Perfect JR, Lang SD, Durack DT.** 1980. Chronic cryptococcal meningitis: a new experimental model in rabbits. Am. J. Pathol. **101:**177–194.
51. **Stajich JE, Harris T, Brunk BP, Brestelli J, Fischer S, Harb OS, Kissinger JC, Li W, Nayak V, Pinney DF, Stoeckert CJ, Roos DS.** 2012. FungiDB:

an integrated functional genomics database for fungi. Nucleic Acids Res. **40:**D675–D681. http://dx.doi.org/10.1093/nar/gkr918.
52. **Cheng S, Clancy CJ, Xu W, Schneider F, Hao B, Mitchell AP, Nguyen MH.** 2013. Profiling of *Candida albicans* gene expression during intra-abdominal candidiasis identifies biologic processes involved in pathogenesis. J. Infect. Dis. **208:**1529–1537. http://dx.doi.org/10.1093/infdis/jit335.
53. **Zhang YE, Landback P, Vibranovski MD, Long M.** 2011. Accelerated recruitment of new brain development genes into the human genome. PLoS Biol. **9:**e1001179. http://dx.doi.org/10.1371/journal.pbio.1001179.
54. **Liu X, Hu G, Panepinto J, Williamson PR.** 2006. Role of a VPS41 homologue in starvation response, intracellular survival and virulence of *Cryptococcus neoformans*. Mol. Microbiol. **61:**1132–1146. http://dx.doi.org/10.1111/j.1365-2958.2006.05299.x.
55. **Sanguinetti M, Posteraro B, La Sorda M, Torelli R, Fiori B, Santangelo R, Delogu G, Fadda G.** 2006. Role of AFR1, an ABC transporter-encoding gene, in the in vivo response to fluconazole and virulence of *Cryptococcus neoformans*. Infect. Immun. **74:**1352–1359. http://dx.doi.org/10.1128/IAI.74.2.1352-1359.2006.
56. **Posteraro B, Sanguinetti M, Sanglard D, La Sorda M, Boccia S, Romano L, Morace G, Fadda G.** 2003. Identification and characterization of a *Cryptococcus neoformans* ATP binding cassette (ABC) transporter-encoding gene, CnAFR1, involved in the resistance to fluconazole. Mol. Microbiol. **47:**357–371. http://dx.doi.org/10.1046/j.1365-2958.2003.03281.x.
57. **Bissinger PH, Kuchler K.** 1994. Molecular cloning and expression of the *Saccharomyces cerevisiae* STS1 gene product. A yeast ABC transporter conferring mycotoxin resistance. J. Biol. Chem. **269:**4180–4186.
58. **Jung KW, Strain AK, Nielsen K, Jung KH, Bahn YS.** 2012. Two cation transporters Ena1 and Nha1 cooperatively modulate ion homeostasis, antifungal drug resistance, and virulence of *Cryptococcus neoformans* via the HOG pathway. Fungal Genet. Biol. **49:**332–345. http://dx.doi.org/10.1016/j.fgb.2012.02.001.
59. **Small JM, Mitchell TG, Wheat RW.** 1986. Strain variation in composition and molecular size of the capsular polysaccharide of *Cryptococcus neoformans* serotype A. Infect. Immun. **54:**735–741.
60. **Monk BC, Goffeau A.** 2008. Outwitting multidrug resistance to antifungals. Science **321:**367–369. http://dx.doi.org/10.1126/science.1159746.
61. **Lengeler KB, Wang P, Cox GM, Perfect JR, Heitman J.** 2000. Identification of the MATa mating-type locus of *Cryptococcus neoformans* reveals a serotype A MATa strain thought to have been extinct. Proc. Natl. Acad. Sci. U. S. A. **97:**14455–14460. http://dx.doi.org/10.1073/pnas.97.26.14455.
62. **Meyer W, Aanensen DM, Boekhout T, Cogliati M, Diaz MR, Esposto MC, Fisher M, Gilgado F, Hagen F, Kaocharoen S, Litvintseva AP, Mitchell TG, Simwami SP, Trilles L, Viviani MA, Kwon-Chung J.** 2009. Consensus multi-locus sequence typing scheme for *Cryptococcus neoformans* and *Cryptococcus gattii*. Med. Mycol. **47:**561–570. http://dx.doi.org/10.1080/13693780902953886.
63. **Larkin MA, Blackshields G, Brown NP, Chenna R, McGettigan PA, McWilliam H, Valentin F, Wallace IM, Wilm A, Lopez R, Thompson JD, Gibson TJ, Higgins DG.** 2007. Clustal W and Clustal X version 2.0. Bioinformatics **23:**2947–2948. http://dx.doi.org/10.1093/bioinformatics/btm404.
64. **Berlocher SH, Swofford DL.** 1997. Searching for phylogenetic trees under the frequency parsimony criterion: an approximation using generalized parsimony. Syst. Biol. **46:**211–215.
65. **Benjamini Y, Hochberg Y.** 1995. Controlling the false discovery rate: a practical and powerful approach to multiple testing. J. R. Stat. Soc. B Stat. Methodol. **57:**289–300.
66. **DePristo MA, Banks E, Poplin R, Garimella KV, Maguire JR, Hartl C, Philippakis AA, del Angel G, Rivas MA, Hanna M, McKenna A, Fennell TJ, Kernytsky AM, Sivachenko AY, Cibulskis K, Gabriel SB, Altshuler D, Daly MJ.** 2011. A framework for variation discovery and genotyping using next-generation DNA sequencing data. Nat. Genet. **43:**491–498. http://dx.doi.org/10.1038/ng.806.
67. **Kent WJ.** 2002. BLAT—the BLAST-like alignment tool. Genome Res. **12:**656–664. http://dx.doi.org/10.1101/gr.229202.